(12)

(12)

Final Report

for

Application of Photorefractive Crystals to Solve Matrix Algebra Problems Optically

Sponsored by

Department of the Navy, Office of Naval Research

Under Contract No. N00014-86-K0697

Grantee

The Regents of the University of California

University of California, San Diego

La Jolla, CA 92093

Principal Investigator:

Sing H. Lee

(619)534-2413

Program Manager:

William Miceli

(703)696-4715

Date:

October 27, 1992

I. Program goal

The goals for the project are to solve matrix algebraic problems at high speed by applying photorefractive crystals in optical processing systems, and to study the photorefractives for such application. Although our interest was primarily on solving matrix algebraic problems, in order to improve system performance we found it important to optimize crystal operation and to improve the photorefractive memory performance. For example, a fast response and large coupling gain bandwidth photorefractive amplifier is required in the matrix inversion system, and high photorefractive efficiency and large storage capacity are required for the correlation matrix-tensor multiplier system.

II. Program Summary

The report will be divided into four sections. Section 2.1 describes an all-optical implementation of an iterative algorithm for matrix inversion. Section 2.2 reports the implementation of a correlation matrix tensor multiplier algorithm in photorefractive crystals. Section 2.3 summaries the results that have been obtained in improving photorefractive performance, which includes 45°-cut $BaTiO_3$, applying electrical field and moving grating on SBN and GaP. Section 2.4 reviews our work on photorefractive memory, which includes circulating memory, incremental recording, orthogonal phase encoding and selective erasure. A list of publications resulted from the research is included at the end of this report.

2.1 Optical implementation of an iterative algorithm for matrix inversion

Many areas of engineering require real-time matrix inversion. It is often found that matrix inversion are time-consuming for digital electronic processors. Therefore, parallel optical processing approaches to the solution are of great interest. Because the solution require iterative algorithms which is difficult to achieve by electronic processors for large size matrices, the use of feedback techniques in optical information processing is extremely important. We have carried out an all-optical implementations of an iterative algorithm for matrix inversion (Ref.1) using a confocal Fabry-Perot system with optical feedback and gain provided by a photorefractive $BaTiO_3$ crystal in the feedback path.

Fig.1 shows the schematic diagram of the matrix inversion processor. Y and X represent input and output vectors of the processor, respectively. In the feedback loop, a

matrix-vector multiplier forms the product AX. The input and output of the processor can be related according to the equation

$$Y \pm AX = X .$$

The output vector of the processor is therefore, given by

$$X = (I \pm A)^{-1} Y = B^{-1} Y .$$

To find the inverse of the matrix B, we incorporate the corresponding matrix $A = I \mp B$ in the optical processor. When the input vector Y is set to zero everywhere except for one element, whose value is normalized to unity, and the position of this unity element in Y is sequentially shifted from the uppermost to the lowermost position, the matrix $B^{-1} = (I - A)^{-1}$ will be generated in real-time at the output, column by column.

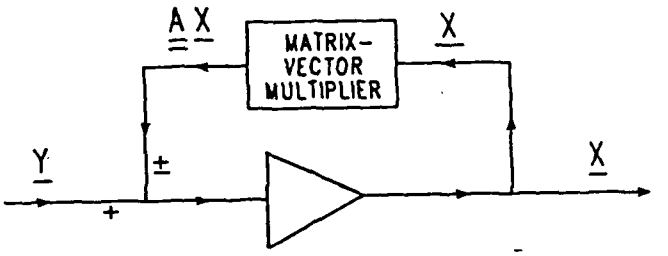

Fig.1 Schematic diagram of the matrix inversion processor showing the matrix-vector multiplier in the feedback loop. Y and X represent (Nx1) input and output vectors respectively.

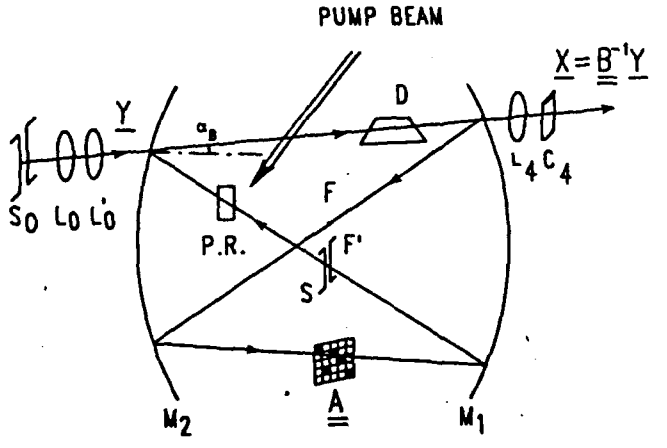

Fig.2. Incorporation of the matrix-vector multiplier and the coherent photorefractive image amplifier into the feedback loop of the confocal Fabry-perot processor made of mirrors M_1 and M_2; L and C are spherical and cylindrical lenses respectively, PR - $BaTiO_3$ Photorefractive crystal D- Dove prism, S - slit.

Fig.2 shows the optical system corresponding to the diagram of Fig.1 for implementing the matrix inversion algorithm, with the matrix-vector multiplier and the photorefractive amplifier incorporated into a confocal Fabry-Perot processor. The input slit S_o which represents the nonzero element of the input vector Y was rotated by the Dove prism D by 90° and was then telecentrically imaged to the matrix mask A by lenses L_o-L_o' and spherical mirror M_1 and M_2. The slit S selects the vertical dc component of the Fourier Transform of AX.. A photorefractive crystal of regular cut $BaTiO_3$ (crystal faces perpendicular to crystal c-axis) was introduced in the feedback loop as a gain media. The output B^{-1} was observed through output lenses L_4C_4 column by column as the input slit S_o is spatially shifted sequentially.

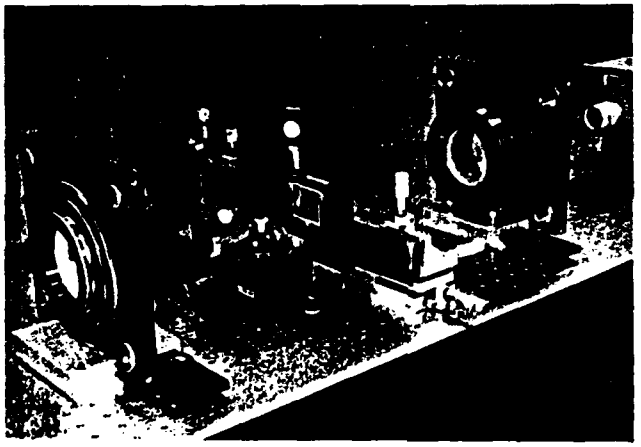

Fig.3. Photograph of the experimental setup. The spatial filters (matrix A and slit S) are inserted into the liquid gate. The mirror on the right is mounted on a piezoelectric translator.

Fig.3 shows the photograph of the experimental setup. One of the two spherical mirrors is mounted on a piezoelectric translator which permits fine adjustment of the mirror spacing allowing the selection of either a positive or negative feedback configuration. A 2-D gray level mask representing matrix A of size 3x3-mm is generated on spectroscopic 649F Kodak film via a computer-controlled scanner. The slit S of width 10 μm is used to ensure the maximum relative error for the matrix-vector multiplier to be < 5%. A single crystal of $BaTiO_3$ was used for coherent image amplification. This amplifier was optimized with respect to such operational characteristics as gain vs space-

bandwidth product and dynamic range. The gain of the photorefractive amplifier is also required to be constant over the entire dynamic range of the matrix **A**. This condition was fulfilled by setting the pump beam intensity much larger than the signal beam intensity. A gray level dynamic range of the order of 100-500 was demonstrated for $BaTiO_3$ crystals. A large space-bandwidth product of 10^6 was also demonstrated; therefore the system has the potential to invert very large size matrices ($10^3 \times 10^3$). Finally, the processing time is independent of the size of the matrix and is only determined by the time response of the crystal, which is inversely proportional to the total incident intensity I_0, typically 0.1-second to 1-second for I_0 = 100 to 10 mW-cm^{-2}.

Experimental verification was performed using an (8 x 8) matrix. Fig.4 shows the experimental result provided by a 3-D plot of the intensity of the output matrix $\mathbf{B}^{-1}$. Comparing with the digital computation result of

$$\mathbf{B}^{-1} = 10^{-2} \times \begin{bmatrix} 127 & 12 & 14 & 9 & 8 & 6 & 8 & 9 \\ 12 & 124 & 14 & 15 & 12 & 11 & 9 & 6 \\ 14 & 14 & 123 & 8 & 6 & 4 & 3 & 5 \\ 9 & 15 & 8 & 124 & 11 & 12 & 15 & 12 \\ 8 & 12 & 6 & 11 & 126 & 9 & 11 & 8 \\ 6 & 11 & 4 & 12 & 9 & 127 & 9 & 6 \\ 8 & 9 & 3 & 15 & 11 & 9 & 129 & 8 \\ 9 & 6 & 4 & 12 & 8 & 6 & 8 & 126 \end{bmatrix},$$

the experimental accuracy is 5%.

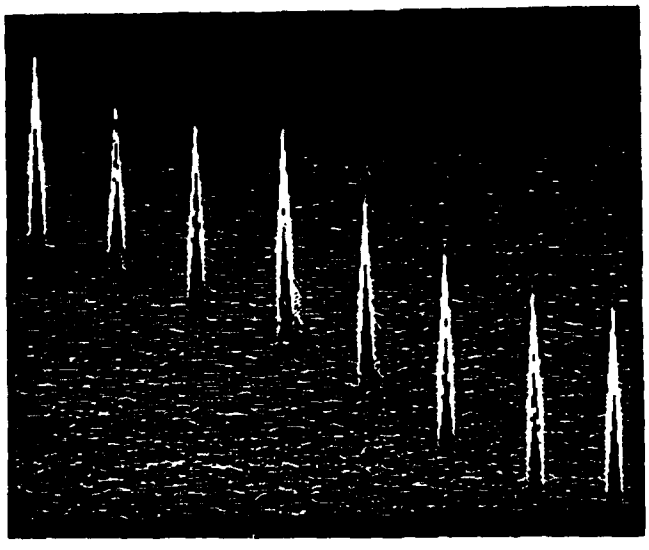

Fig.4. Experimental result of the inverted matrix $\mathbf{B}^{-1}$ represented in three-dimension.

2.2 Optical Implementation of Correlation Matrix-Tensor Multiplier Algorithm

Matrix-tensor multiplication has many important applications, including interconnection between 2-D data arrays for digital and neural computing. For NxN input and output arrays, the interconnection tensor is 4th rank containing the N^4 independent values .

We have built a correlation matrix-tensor multiplier (CMTM) that can implement an arbitrary complex-weighted 2-D array interconnection. In the CMTM system, the 2-D input was transmitted through a phase-code mask and correlated with a control image constructed from the interconnection weights. The optical correlation was performed by either photorefractive real-time four-wave mixing or by pre-storing the interconnection weight in the crystal. Because the real-time four-wave mixing is limited by slow photorefractive response (Ref.3), we chose to use the late version for implementation. Multiple interconnection patterns were prestored as color-multiplexed volume reflection holograms in z-cut $LiNbO_3$. Fast reconfiguration between interconnection patterns is possible using a wavelength tunable source, decoupling both the modulation and switching speeds from slow photorefractive response. The CMTM algorithm allows for graceful accommodation of limited spatial light modulator size needed to input the control tensor by trading-off output signal-to-noise ratio for reduced control tensor bandwidth requirement.(Ref.2) Experimental results confirmed theoretical predictions that the CMTM system works best for densely connected networks, with a large fan-in to each output. Interconnection of up to 4096 inputs and outputs was demonstrated using such dense interconnection patterns. An aggregate average SNR of over 200 was obtained for 1024 inputs and outputs. Fig.5 shows the output for different input array size (N^2) and phase-code density k. The connection tensor size was 1000x1000 pixels (25-mm square), approaching the realistic maximum for an optical system to resolve with good accuracy. The overall results match the theoretical prediction.

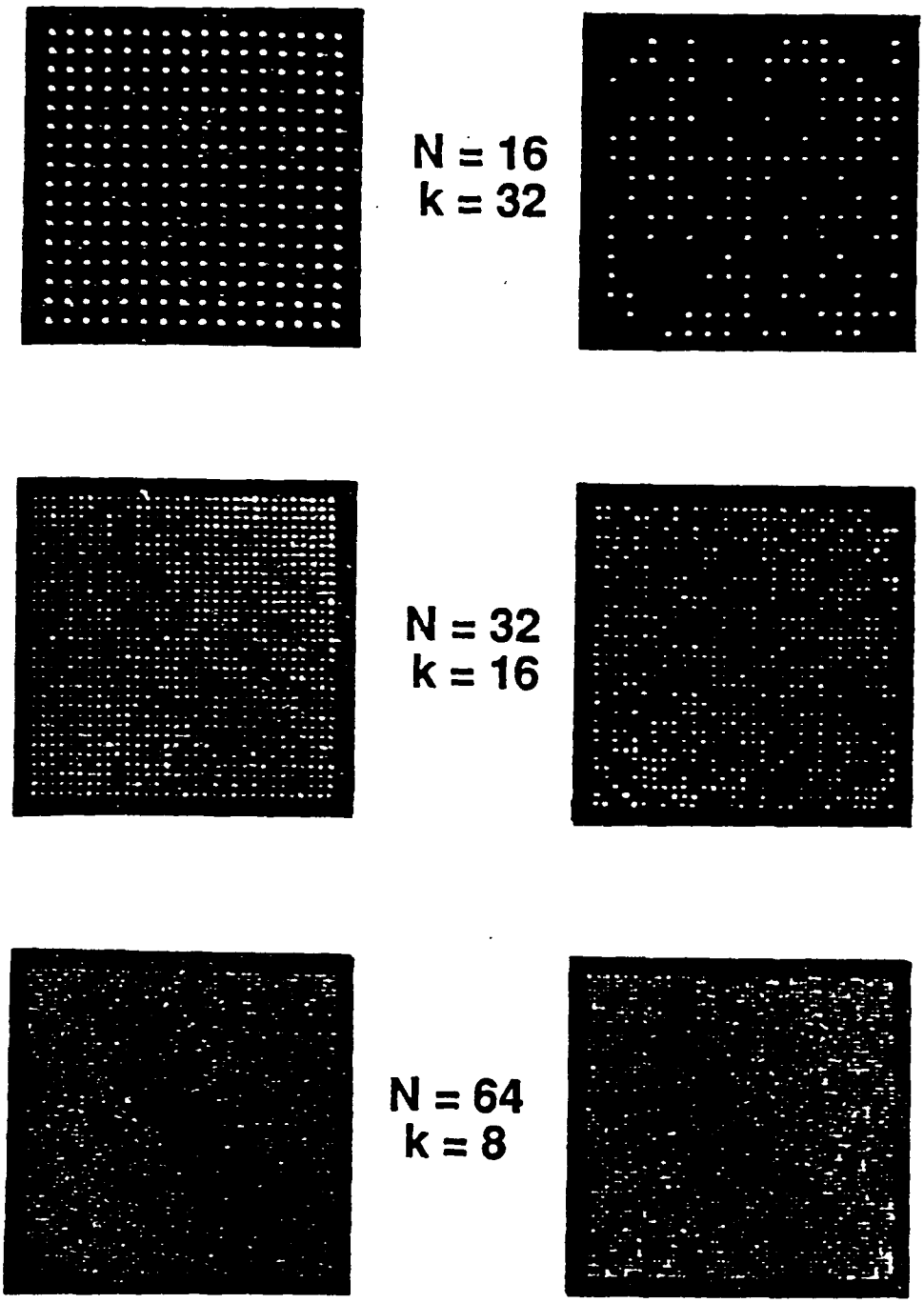

Fig.5. Effect of array size on output SNR. The control image SBP was held at about 1000x1000 by decreasing k linearly with N. At left, all the inputs are on. At right, half the inputs are masked. Output SNR decreased as N2 grows from 256 to 1024 to 4096.

2.3 Techniques developed at UCSD for improving photorefractive performance

The system performance of both matrix inversion and CMTM strongly relay upon the photorefractive operation. For example, a fast response and large coupling gain bandwidth photorefractive amplifier is required in the matrix inversion system, and high photorefractive diffraction efficiency and large storage capacity are required in the CMTM system. In the following we summarize some of the techniques of photorefractive performance improvement developed at UCSD under the support of this contract.

2.3.1 Enhanced photorefractive performance from 45°-cut $BaTiO_3$

$BaTiO_3$ photorefractive amplifier is one of the key elements in the matrix inversion implementation reported in section 2.1. In this implementation, the $BaTiO_3$ is a conventional cut with its faces polished perpendicular to the crystal optic axis c. In order to improve the system performance such as gain, response time and uniformity, we proposed and have demonstrated that changing the crystal cut of $BaTiO_3$ to 45° to c can provide superior photorefractive performance to our system applications.(Ref.3) It increases the achievable gain coefficient, reduces the response time, and changes the gain and index modulation response as a function of external input angles.

We characterized the photorefractive performance of a 45°-cut $BaTiO_3$ and compared it with the conventional 0°-cut material. The achievable peak gain coefficient Γ is increased to a value of 26 cm^{-1}, while Γ for a conventional $BaTiO_3$ is only 12 cm^{-1}. The strong fanning observed in thicker 45° crystal reduces the effective Γ for two-wave mixing but can be applied to enhance the performance of the crystal in certain photorefractive applications which use the fanning effect to their advantage. Two examples of these are self-pumped phase conjugation and fanning-based novelty filtering (Ref.4). The angular dependence of Γ on the input beam angles is flatter in the 45°-cut crystal, resulting in more uniform amplification over a wide range of input beam angles. The response times measured in 45°-cut crystal were 1 order of magnitude faster than similar 0°-cut crystals. Application of an external electric field can slightly increase Γ, but does not reduce the response time and can damage the crystal.

2.3.2. Increased multiplex hologram capacity of SBN with applied field

Increasing storage capacity of photorefractive materials is very important for improving the CMTM performance because more interconnection patterns can be prestored and accessed at very high speed. We have characterized the performance of photorefractive $Sr_{0.6}Ba_{0.4}Nb_2O_6$ under an externally applied electric field. We

demonstrated that the volume multiplexing capacity increases substantially by using an applied dc field.(Ref.5) In a 1-mm-thick crystal the number of 2% diffraction efficiency holograms increased from 4 to 32 at an external field of 14 kV/cm. The minimum diffraction efficiency for 30 holograms increased from 2.4% to 5.4% at 12.6kV/cm field. Accurate prediction of photorefractive performance under an applied field can be made with material parameters measured at zero applied field. The field dependence of the gain coefficient, response time, sensitivity, and diffraction efficiency were obtained and fit very well with the theoretical prediction calculated using Kukhtarev's photorefractive material equation. Optimum crystal operation conditions of applied field and grating period were obtained.

2.3.3. Moving grating for enhanced holographic recording in SBN

Energy coupling during holographic recording in thick SBN (e.g. 5-mm) tends to reduce the beam ratio of 1 at the input to 10^{-7} at the exit face. This greatly limits the usable crystal thickness reducing the diffraction efficiency and storage capacity which are required by many applications, including CMTM. We have demonstrated that holographic recording can be improved by using a moving grating to reduce energy coupling.(Ref.6) In Ce-doped $Sr_{0.6}Ba_{0.4}Nb_2O_6$ under an applied dc electric field, experimental and theoretical results show that the proper grating velocity can maximize the modulus and the real part of the space-charge field while reducing the imaginary component of the space-charge field (and energy coupling) to zero. Avoiding energy transfer between the recording beams allows us to maintain maximum contrast throughout the crystal, producing a uniform, high-index-modulation grating with enhanced diffraction efficiency and superposition properties. We demonstrated that with an applied field of 5.3kV/cm, the peak diffraction efficiency was increased from 58% to 93% by choosing an optimum moving grating velocity which minimized coupling.

2.3.4. Moving grating for enhanced beam-coupling and phase-conjugation in GaP

The ferroelectric photorefractive materials, such as $BaTiO_3$, SBN and $LiNbO_3$ possess slow time response, affecting the speed of both matrix inversion system and real-time CMTM system. In order to improve the system operating speed, we explored new photorefractive materials with fast time response. It has been shown that semiconductor photorefractive materials provide response time much fast than that of ferroelectric materials, among which GaP is particularly attractive because it operates in the spectral range of 0.6 to 0.9 μm. However, weak photorefractive effect in GaP has been limiting its applications. We have demonstrated a technique to enhanced photorefractive effect in

GaP by using a dc field and a moving grating at laser wavelength of 633nm. Two-beam coupling gain coefficient Γ was increased from 0.3 cm^{-1} to 2.5 cm^{-1} and the transient phase-conjugate reflectivity was increased from 0.3% to 4.5% by applying a dc field of 16.7 kV/cm and choosing the optimum fringe velocity. The experimental results are found in good agreement with the theoretical predictions.(Ref.7)

2.4 Photorefractive Memory

3-D photorefractive memories offer the advantages of high storage density, distributed storage, and fast parallel access. These characteristics have been applied to our CMTM system (Section 2.2) and many other parallel opto-electronic processing applications. The high performance of 3-D photorefractive memories rely on various basic requirements, such as fast random access time, read/write/erase capabilities, high angular and wavelength selectivity, high resolution, large and uniform diffraction efficiency, long storage time and nondestructive readout, which are still the research topics and are extremely important to our CMTM system performance. In this section, we will review the related research projects which have been accomplished at UCSD during the last few years.

2.4.1. Dynamic circulating photorefractive memory

The objective of this project is to construct a dynamic photorefractive memory that provides (1) nondestructive readout, i.e., after many readings, the memory can be refreshed by rewriting the still-useful information from one crystal into the other, and (2) write-erase capability, i.e., while rewriting the useful part of the information from one crystal to the other, we also can replace obsolete information that must be erased by new information introduced from the memory input. For accomplishing this task, we proposed and have implemented an architectural approach using dynamic 3-D volume storage that circulates holograms between two photorefractive crystals.(Ref.8)

In our architecture the input images are stored sequentially in one of the two crystals (i.e., PRC1) until the total memory capacity of that crystal is reached. After many readouts the stored information in PRC1 will be degraded. We then transfer the useful part of the information from PRC1 to the second crystal PRC2. If the storage capacity of PRC2 is not reached after transfer, additional input images can be recorded in PRC2. The first crystal is then optically erased to prepare it for the next transfer cycle. The two crystals are functionally identical, exchanging tasks periodically. In order to increase the effective write-erase asymmetry of the crystal and amplify the recalled images, an optical amplifier (LCLV) was introduced into the system. We demonstrated transfer of a single

image (pixel size 400 μm) between two crystals. No noticeable degradation in the pixel quality was observed after more than fifteen transfers with the average SNR better than 86. This experiment shown that our circulating memory architecture provides write-erase storage capacity with robustness to multiple optical readouts.

2.4.2. Incremental recording and orthogonal phase codes for photorefractive hologram multiplexing

The commonly used schedule recording technique for photorefractive hologram superposition involves a complicated recording procedure with a long first exposure followed by shorter and shorter exposures. The schedule is calculated from the material's response times and the maximum attainable index modulation. A small error in material characterization (also nonuniformities or changes in material characteristics) can result in highly nonuniform diffraction efficiencies. Also problems of fanning and beam coupling will be dominant in the long initial exposures, which tend to restrict the maximum attainable index modulation to well below the theoretical value. We have demonstrated a new recording schedule called incremental recording by which the problems associated with the schedule recording can be avoided. We have studied the effects of the incremental recording approach on holographic storage, and the criteria for choosing appropriate recording parameters. In this approach, the diffraction efficiency uniformity dependents only on Δt but not on material parameters. Therefore, by using incremental recording it is much easier to reach uniform diffraction efficiency than by using schedule recording (Ref.9).

In incremental recording, each of N holograms is recorded with a series of exposures Δt, each extremely short compared with the material's response time. During recording, each image and reference pair is sequentially displayed, repetitively cycling through all N images. The first recorded hologram will remain after incrementing the other (N-1) holograms because small index modulation possess high writing and low erasing sensitivity. As this process is repeated, all the holograms' diffraction efficiencies gradually increase until the recording process reaches saturation, i.e., when index gained during recording increment equals to that erased during (N-1) erasures when the holograms are being recorded.

In incremental recording approach, the recording system must repeatedly display the input and reference image pairs, reproducing the interference pattern to within much less than one fringe width. To achieve this we have developed a method of addressing called orthogonal phase encoding by which different holograms can be recorded and addressed without mechanical movement. In orthogonal phase encoding approach the reference

wave fronts are generated by displaying a set of orthogonal phase codes on a phase-modulator array. Each hologram is recorded (addressed) by one of the set of phase coded plane waves. The phase codes are chosen such that the inner product of one code with any other code from the set is zero, that is , they are orthogonal to each other. When the crystal is illuminated with one phase code, the unwanted cross terms from the other holograms interfere destructively in the volume of the crystal, while the output recorded with that phase code interference constructively to produce a full-intensity reconstruction. In general, a phase-modulator with M pixels provides M orthogonal phase codes. In the particular case of $M = 2^k$, the solution is a set of binary phase codes equivalent to the bipolar Walsh function. These codes can be generated from a $k = \log_2 M$ bit address, therefore this phase-encoding technique is useful for fast parallel access, especially when a smart spatial light phase modulator with local electronic logic is used.

The combination of incremental recording and binary orthogonal phase codes was demonstrated experimentally. We tested the orthogonality of codes by incrementally recording 16 images in a 1-mm-thick Fe-doped $LiNbO_3$ crystal. The cross talk between the images was low, providing an average SNR of 100:1. We also investigated the signal uniformity for the incremental recording by varying the incremental exposure time. As expected by our theoretical prediction, the signal uniformity is significantly improved with a reduced recording increment. The storage capacity of the incremental recording procedure is identical to that of the schedule recording.

2.4.3. Selective erasure for dynamic photorefractive memory

Applications of photorefractive memory require not only robust readout capability and uniform diffraction efficiency with high signal fidelity which are the subject of Section 2.4.1 and Section 2.4.2 respectively, but also fast update capability for such applications as neural networks. The simple way of incoherent erasure which has been commonly used is too slow, while selective erasure based on superimposed recording of a π-phase-shifted image onto the old image has been reported to be much faster than the incoherent erasure. The objective of this project is to analyze the dynamics of the selective erasure process and to apply it to a dynamic photorefractive memory.

We derived a theoretical equation of the dynamics of the index distribution for selective erasure process by using photorefractive material equations. This equation can be used to predict the diffraction efficiency versus erasure time and selective erasure time (the time for completely erasing the hologram) versus initial refractive index modulation. It was shown that selective erasure process is much faster than incoherent erasure process. Experimental results show good agreement with theoretical prediction.(Ref.10)

We have applied the selective erasure process together with the incremental recording schedule (Section 2.4.2) to the dynamic photorefractive optical memory. Four pages of information were stored in a 1-mm-thick Ce-doped $Sr_{0.6}Ba_{0.4}Nb_2O_6$ by incremental recording to reach saturation. Fig.6 shows the experimental demonstration of selective erasure process. One of the four recorded binary images of the letter (U, C, S, D) [see Fig.6(a)] D was selectively erased [see Fig.6(b)] and was replaced by a C [see Fig.6(c)]. It took only a few seconds to completely selective erase one page and another 20-30 seconds to recording a new page and circulating all the pages until reach saturated diffraction efficiency. The experiments lemonstrated the robust readout and fast read/write/erase capability (Ref.11,12).

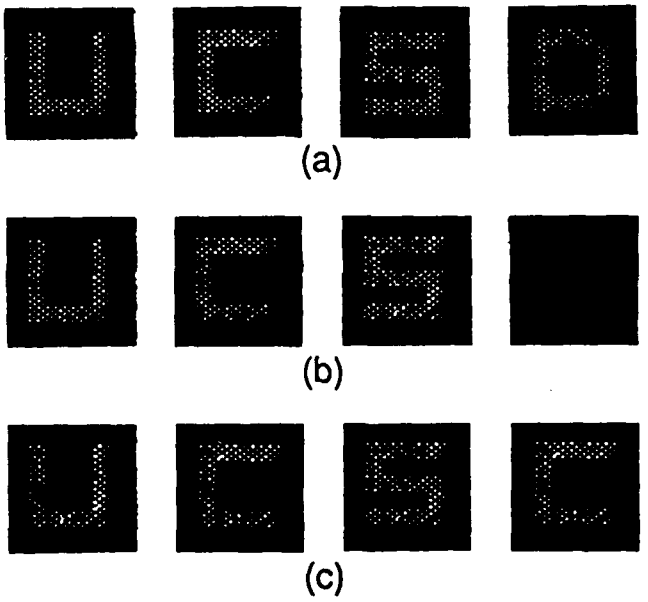

Fig.6. Photographs of stored binary images (a) before selective erasure, (b) after selective erasure, (c) after image update.

III. Conclusion and Future Works

We have demonstrated an all-optical implementation of an iterative algorithm for matrix inversion and 32x32 interconnection by using correlation matrix-tensor multiplier algorithm. We made several contributions to photorefractive performance improvement, which includes enhanced gain and response time using 45°-cut $BaTiO_3$, increased holographic capacity by applying dc field on SBN, increased diffraction efficiency in

SBN by applying moving grating, and enhanced gain and phase-conjugation in GaP by applying dc field and moving gratirg. For photorefractive memory, we have introduced solutions to some of the most serious problems such as nondestructive readout, write/erase/rewrite capability, uniformity of diffraction efficiency and fast random access by demonstrating dynamic circulating memory, incremental recording, orthogonal phase encoding address and selective erasure.

Our future work will be more concentrated on applying photorefractive materials for packaging of opto-electronic system such as neural networks and optical interconnection systems in order to fully use the in-situ recording nature of the photorefractives for self-alignment and adaptability.

Reference (Publications resulted from the research carried out from this Contract/Grant)

[1] H. Rajbenbach, Y. Fainman, and S. H. Lee; "Optical implementation of iterative algorithm for matrix inversion"; *Applied Optics*, **26**, 1024-1031, 1987.

[2] J. E. Ford, Y. Fainman, and S. H. Lee; "Array interconnection by phase coded optical correlation"; *Optics Letters*, **15**, 1088-1090, 1990.

[3] J. E. Ford, Y. Fainman, and S. H. Lee; "Enhanced photorefractive performance from 45^{o} -cut $BaTiO_3$" *Applied Optics*, **28**, 4808-4815, 1989.

[4] J. E. Ford, Y. Fainman, and S. H. Lee; "Time-integrating interferometry using photorefractive fanout"; *Optics Letters*, **13**, 856-858, 1988.

[5] J. E. Ford, J. Ma, Y. Fainman, S. H. Lee, Y. Taketomi, D. Bize, and R. R. Neurgaonkar; "Multiplex holography in strontium barium niobate with applied field"; *Journal of the Optical Society of America*, **A9**, 1183-1192, 1992.

[6] J. Ma, J. E. Ford, Y. Taketomi, and S. H. Lee; "Moving grating for enhanced holographic recording in cerium-doped $Sr_{0.6}Ba_{0.4}Nb_2O_6$"; *Optics Letters*, **16**, 270-272, 1991

[7] J. Ma, Y. Taketomi, Y. Fainman, J. E. Ford, S. H. Lee and K. Chino; "Moving grating and dc external field in photorefractive GaP at 633 nm"; *Optics Letters*, **16**, 1080-1082, 1991.

[8] H. Sasaki, Y, Fainman, J. E. Ford, Y. Taketomi, and S. H. Lee; "Dynamic photorefractive optical memory"; *Optics Letters*, **16,** 1874-1876, 1991.

[9] Y. Taketomi, J. E. Ford, H. Sasaki, J. Ma, Y. Fainman, S. H. Lee; "Incremental recording for photorefractive hologram multiplexing"; *Optics Letters*, **16,** 1774-1776, 1991.

[10] H. Sasaki, J. Ma, Y. Fainman, and S. H. Lee; "Selective erasure for dynamic photorefractive memory"; ***CLEO'92*** at Anaheim, CA. (May, 1992)

[11] H. Sasaki, J. Ma, Y. Fainman, and S. H. Lee; "Dynamics of composite grating in photorefractive SBN:60"; *1992 OSA Topical Meeting on Nonlinear Optics, Fundamentals, Applications*, Maui, Hawaii (Aug. 1992).

[12] H. Sasaki, J. Ma, Y. Fainman, S. H. Lee and Y. Taketomi; "Fast update of dynamic photorefravtive optical memory"; *Optics Letters*, **17**, 1468-1470, 1992.

SUPPLEMENTARY

INFORMATION

UNIVERSITY OF CALIFORNIA, SAN DIEGO

BERKELEY • DAVIS • IRVINE • LOS ANGELES • RIVERSIDE • SAN DIEGO • SAN FRANCISCO

SANTA BARBARA • SANTA CRUZ

DEPARTMENT OF ELECTRICAL & COMPUTER ENGINEERING, 0407

LA JOLLA, CALIFORNIA 92093-0407

Dr.Sing H. Lee
Ph (619) 534 2413
Fax (619) 534 1225

December 15, 1992

Defence Technical Information Center
Bldg.5, Cameron Station
Alexandria, VA 22314

Dear Sir:

Enclosed please find the completed Form 298 which should have been sent together with our Final Report for ONR Grant No. N00014-86-K0697 on Dec.3, 1992.

Sincerely yours,

Sing H. Lee
Professor

Enclosure

REPORT DOCUMENTATION PAGE

Form Approved
OMB No. 0704-0188

1. AGENCY USE ONLY (Leave blank)	2. REPORT DATE	3. REPORT TYPE AND DATES COVERED
	October 27, 1992	June 1, 1986 to October 27, 1992

4. TITLE AND SUBTITLE

Application of Photorefractive Crystals to Solve Matrix Algebra Problems Optically

5. FUNDING NUMBERS

Contract No.
N00014-86-K0697

6. AUTHOR(S)

Sing H. Lee

7. PERFORMING ORGANIZATION NAME(S) AND ADDRESS(ES)

Department of Electrical & Computer Engineering
University of California, San Diego
La Jolla, CA 92093-0407

8. PERFORMING ORGANIZATION REPORT NUMBER

9. SPONSORING/MONITORING AGENCY NAME(S) AND ADDRESS(ES)

Department of Navy, Office of Naval Research
800 North Quincy Street
Arlington, Virginia 22217-5000

10. SPONSORING/MONITORING AGENCY REPORT NUMBER

11. SUPPLEMENTARY NOTES

12a. DISTRIBUTION/AVAILABILITY STATEMENT

12b. DISTRIBUTION CODE

13. ABSTRACT *(Maximum 200 words)*

We have demonstrated an all-optical implementation of an iterative algorithm for matrix inversion and optical interconnection between 32x32 arrays by using correlation matrix-tensor multiplier algorithm. In order to improve the performance of the matrix inversion system, we made several contributions to improve photorefractive performance, which includes enhanced gain and response time using 45^{o}-cut $BaTiO_3$, increased holographic capacity by applying dc field on SBN, increased diffraction efficiency in SBN by applying moving grating, and enhanced gain and phase-conjugation in GaP by applying dc field and moving grating. In order to improve the performance of the correlation matrix-tensor multiplier, we have solved some of the photorefractive problems such as destructive readout, write/erase/rewrite capability, non-uniformity of diffraction efficiency and slow random access, by demonstrating dynamic circulating memory, incremental recording, orthogonal phase encoding address and selective erasure.

14. SUBJECT TERMS	15. NUMBER OF PAGES
Photorefractive Applications, Matrix Algebra Matrix-tensor Multiplier	14
	16. PRICE CODE

17. SECURITY CLASSIFICATION OF REPORT	18. SECURITY CLASSIFICATION OF THIS PAGE	19. SECURITY CLASSIFICATION OF ABSTRACT	20. LIMITATION OF ABSTRACT
UNCLASSIFIED	UNCLASSIFIED	UNCLASSIFIED	SAR